

Seamless Hourly AOD Fusion Based on Himawari Satellite and Reanalysis Data

Meng Wu^{1,2}, Ning Wang^{1,*}

¹*Aerospace Information Research Institute, Chinese Academy of Sciences, 100094, Beijing, China*

²*University of Chinese Academy of Sciences, 100049, Beijing, China*

**Corresponding author*

Keywords: Aerosol Optical Depth (AOD); Himawari satellite; Optimal Interpolation; Hourly seamless product

Abstract: Aerosol Optical Depth (AOD) is a key parameter for characterizing the total columnar aerosol load in the atmosphere, which is of great significance for climate change research, air quality monitoring, and global radiation budget assessment. Geostationary satellites can provide high-frequency hourly observations and have unique advantages in capturing rapid intra-day variations of aerosols. However, their AOD products generally suffer from large-scale spatiotemporal gaps due to factors such as cloud cover and high surface albedo, and a single product often struggles to balance accuracy and coverage simultaneously. To address this issue, this paper focuses on East Asia (20°N-50°N, 100°E-150°E) and utilizes three Himawari L3 hourly AOD products (AOT_L2_Mean, AOT_Merged, AOT_Pure) together with MERRA-2 reanalysis AOD data as data sources. A seamless hourly AOD fusion framework is constructed using the Optimal Interpolation method. Firstly, based on AERONET ground-based observations, the accuracy and coverage of the four products are validated and analyzed, clarifying their error characteristics and complementary relationships. Secondly, based on the validation accuracy of the three Himawari products and MERRA-2, the products are fused sequentially according to their accuracy levels. A 3×3 neighborhood spatial consistency constraint is introduced to suppress fusion noise, generating a seamless hourly AOD product that balances accuracy and coverage. Experimental results show that among the three Himawari products, AOT_Pure has the highest accuracy ($r=0.807$, RMSE=0.077) but the lowest coverage, while AOT_L2_Mean has the highest coverage but lower accuracy ($r=0.662$, RMSE=0.158). The MERRA-2 product offers the advantage of spatiotemporal continuity but has limited accuracy ($r=0.617$, RMSE=0.121). The fused product achieves 100% spatiotemporal seamless coverage while demonstrating higher accuracy compared to the MERRA-2 AOD product ($r=0.662$, RMSE=0.118, EE ratio 68.4%) and retains the local detailed features of the original Himawari observations. The fused product effectively fills daytime cloud-induced gaps and nighttime observation blind areas, providing reliable data support for dynamic monitoring of pollution processes and air quality research in East Asia.

1. Introduction

Aerosol Optical Depth (AOD) is a key parameter for characterizing the total columnar aerosol load in the atmosphere, which is of great significance for climate change research, air quality monitoring, and global radiation budget assessment [1]. Compared with polar-orbiting satellites, geostationary satellites can perform high-frequency continuous observations over fixed areas and have unique advantages in capturing rapid intra-day variations of aerosols and tracking the evolution of pollution events. Geostationary satellites, represented by the Himawari series, equipped with the advanced AHI imager, can provide high-frequency observations every 10 minutes and generate operational hourly AOD products, providing valuable data sources for dynamic aerosol monitoring in East Asia [2].

However, affected by factors such as cloud cover, high surface albedo, and large solar zenith angles, Himawari hourly AOD products generally suffer from large-scale spatiotemporal gaps. Especially in cloudy areas, nighttime periods, and high-latitude regions, the proportion of effective observational data is significantly reduced, severely restricting their application in continuous time series analysis [3]. At the same time, due to the limitations of retrieval algorithms, a single satellite product often struggles to balance accuracy and coverage simultaneously. For example, the officially released AOT_L2_Mean product has relatively high coverage but lower accuracy, while the AOT_Pure product has high accuracy but limited coverage. Therefore, how to fully utilize the complementary information of multi-source data to achieve high-precision, seamless fusion of hourly AOD products has become one of the research hotspots in current geostationary satellite aerosol remote sensing applications [4].

In recent years, scholars worldwide have conducted extensive research on AOD data fusion. Multi-source data fusion methods mainly include weighted averaging, Bayesian Maximum Entropy, and Optimal Interpolation. Among them, the Optimal Interpolation (OI) method, due to its solid theoretical foundation and high computational efficiency, is widely used in numerical weather prediction and multi-source remote sensing data fusion [5, 6]. This method estimates the optimal analysis value in the sense of minimum variance by introducing background field error covariance and observation error covariance, effectively fusing products with different accuracy and coverage characteristics to achieve complementary advantages.

Currently, fusion research on geostationary satellite AOD products mainly focuses on daily-scale products, while seamless fusion on an hourly scale is still relatively rare. Moreover, existing studies rarely jointly fuse multiple Himawari official products with reanalysis AOD (such as MERRA-2) to simultaneously improve data accuracy and spatiotemporal continuity. The MERRA-2 reanalysis AOD product, developed by NASA's Global Modeling and Assimilation Office, has the advantages of spatiotemporal continuity and global coverage, providing reliable background field information for areas missing satellite data.

Based on the above background, this paper takes East Asia as the study area, uses three Himawari hourly AOD products and MERRA-2 hourly AOD reanalysis data as data sources, and adopts the Optimal Interpolation fusion method to construct a seamless hourly AOD fusion product. This paper first validates and analyzes the accuracy and coverage of the three Himawari products and the MERRA-2 product. Secondly, based on the OI method, a fusion framework is established, combining the error statistical information of multi-source products with spatial neighborhood consistency to generate an hourly AOD fusion field that balances accuracy and coverage. Finally, the accuracy of the fusion results is evaluated using AERONET ground-based observation data to verify the effectiveness of the method. This study aims to provide high spatiotemporal continuity AOD data support for regional air quality monitoring, dynamic tracking of pollution processes, and climate change research.

2. Study Area and Datasets

2.1. Study Area

The Himawari satellite is positioned in a geostationary orbit at 140.7 °E. To fully leverage the high-frequency observation advantages of the Himawari satellite and validate the effectiveness of the proposed hourly fusion method, this study selects East Asia as the study area, specifically ranging from 20 °N to 50 °N latitude and 100 °E to 150 °E longitude. This area covers the eastern coastal regions of China, the Korean Peninsula, the Japanese archipelago, and parts of the western Pacific Ocean. It is a typical region influenced by the East Asian monsoon, with dense populations, developed industries, and frequent aerosol pollution events. The pollution types are complex, including industrial pollution, biomass burning, and dust. It is highly representative for studying the short-term variation characteristics of AOD. The study period covers the hourly data for January 2024 , as shown in Figure 1.

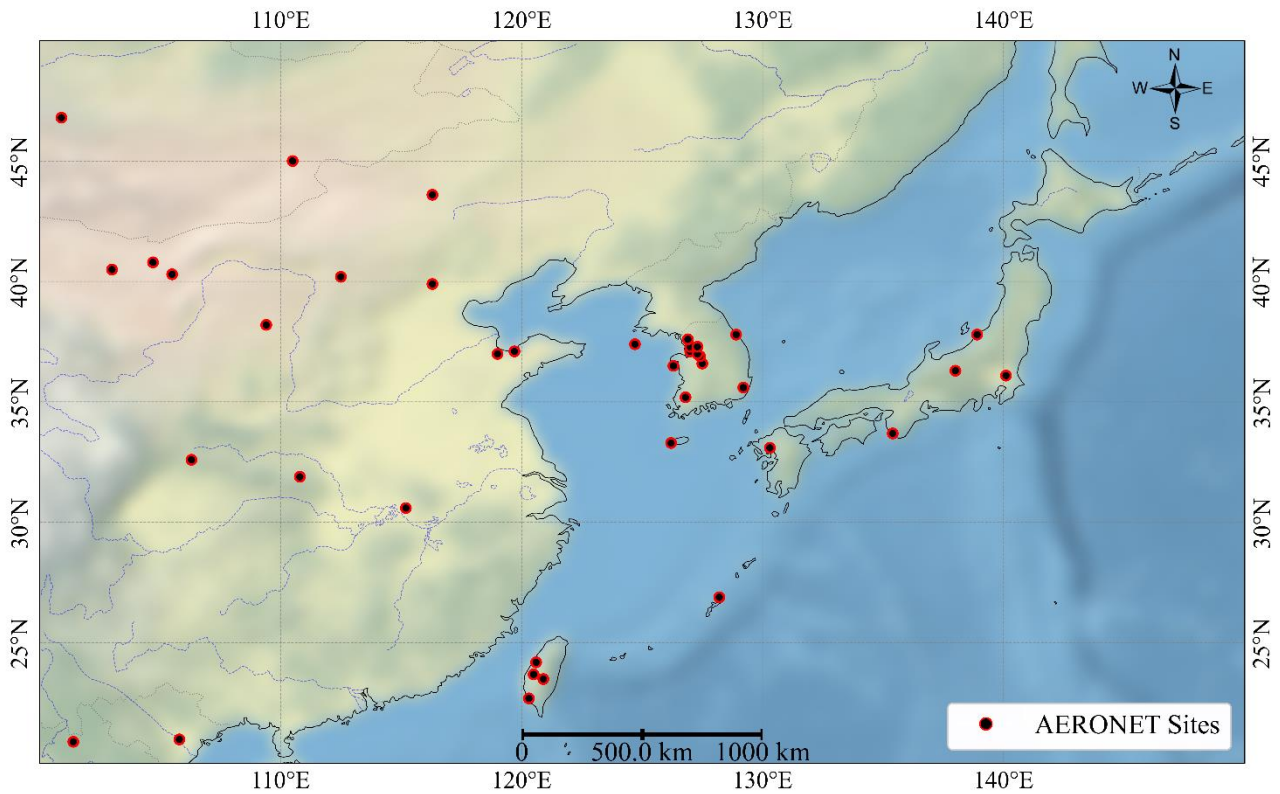


Figure 1: Study Area and Distribution of AERONET Sites

2.2. Experimental Data

2.2.1. Himawari Dataset

Himawari is a new generation of geostationary meteorological satellite operated by the Japan Meteorological Agency, equipped with the advanced AHI (Advanced Himawari Imager), providing unprecedented high spatiotemporal resolution data for aerosol monitoring in the Asia-Pacific region. Himawari-8 was launched in October 2014 and officially entered operational service in July 2015. Himawari-9 was launched in 2016 as an on-orbit backup satellite and is also currently operational. The two satellites together ensure the long-term continuity and stability of the observation series [2].

The AHI sensor is the core payload of the Himawari series satellites, comprising a total of 16

spectral channels covering a wide range from visible to thermal infrared. Among them, the spatial resolution of the visible bands (0.47 μm , 0.51 μm , 0.64 μm) reaches 1km, 1km, and 0.5km respectively, while the spatial resolution for near-infrared and thermal infrared bands is mainly 2km. This multi-band, multi-resolution observation capability makes it suitable not only for aerosol retrieval but also widely applicable in fields such as cloud detection, sea surface temperature retrieval, and vegetation monitoring [2]. The AHI sensor has high design similarity with GOES-R/ABI, representing the international advanced level of current geostationary meteorological satellite imagers.

Based on AHI observation data, the Japan Aerospace Exploration Agency (JAXA) releases official L2 (10-minute) and L3 (hourly) aerosol products. The L3 hourly AOD products include three main types: AOD_L2_Mean, AOD_Pure, and AOD_Merged. AOD_L2_Mean is a simple hourly average of the L2 10-minute products, aggregated only in time without other optimization or correction. AOD_Pure is a more reliable satellite retrieval result obtained through an improved spatiotemporal retrieval algorithm, representing high-quality retrieval values identified by the algorithm. AOD_Merged is the officially released fusion product, which integrates satellite retrieval results and climatological background information, performing post-processing correction and optimization on the satellite AOD product.

Tan et al. conducted a systematic evaluation of Himawari-8 L3 V31 aerosol products over Japan. The results showed that the AOD_Merged product performed best among the three, effectively tracking the spatiotemporal variation characteristics of aerosols in Japan, with higher AOD in spring and summer and lower in autumn and winter. Comparison with AERONET ground-based observations showed that AOD_Merged performed optimally on an hourly scale, although there was a certain degree of systematic overestimation [4].

This paper selects the three L3 hourly AOD products from the Himawari satellite for January 2024. Since the provided products are AOD values at the 500nm band, they are converted to the 550nm band using the following formula:

$$\ln(\tau_0) = \ln(\tau_1) - \alpha \ln\left(\frac{\lambda_0}{\lambda_1}\right) \quad (1)$$

Where τ_0 and τ_1 represent the AOD at wavelengths λ_0 (550nm) and λ_1 (500nm), respectively, and α is the Ångström exponent from the Himawari L3 product.

2.2.2. MERRA-2 Dataset

Table 1: The experimental datasets

Dataset	Data Name	Temporal Resolution	Spatial Resolution
Himawari	AOD_L2_Mean	1h	0.05 °×0.05 °
	AOD_Pure	1h	0.05 °×0.05 °
	AOD_Merged	1h	0.05 °×0.05 °
MERRA-2	MERRA-2 AOD	1h	0.5 °×0.625 °

MERRA-2 (Modern-Era Retrospective analysis for Research and Applications, Version 2) is a global atmospheric reanalysis dataset developed by NASA's Global Modeling and Assimilation Office. Its AOD product, generated by integrating multi-source observational data with an advanced atmospheric chemistry transport model, provides spatiotemporally continuous aerosol distribution information [7]. This study uses the hourly MERRA-2 AOD data for January 2024 as one of the fusion parameters, leveraging its spatiotemporal continuity to assist in AOD fusion. Its spatial resolution is 0.5 °×0.625 °, and the core analysis band is 550nm. The experimental datasets used in this study are summarized in Table 1.

2.2.3. AERONET Dataset

The Aerosol Robotic Network (AERONET), jointly established by the National Aeronautics and Space Administration (NASA) and the French National Centre for Scientific Research (CNRS), is a global ground-based aerosol monitoring network. It provides high-precision AOD measurements using standardized sun photometers. Comprising nearly a thousand sites distributed worldwide, the AERONET network captures the spectral dependence characteristics of aerosols. These sites deliver accurate AOD measurements at approximately 15-minute intervals across the 340–1640 nm range, with an uncertainty of about 0.01–0.02. These data are widely recognized as the "ground truth" for validating satellite-derived AOD estimates [8-9]. This study adopts globally available Level 1.5 quality-assured AERONET data for January 2024 to validate satellite and reanalysis AOD. To match the 550nm band, the Ångström-exponent-based band conversion method is used to obtain 550 nm AOD from AERONET's original channels; the band relationship follows the equation below:

$$\tau_a(\lambda) = k \cdot \lambda^{-a} \quad (2)$$

In the equation, k represents the atmospheric turbidity coefficient, which can be approximated by the aerosol optical depth at 1020 nm. The Ångström exponent a is derived through nonlinear fitting of AOD values at five wavelengths (1020 nm, 870 nm, 670 nm, 500 nm, and 440 nm), yielding both k and a , which are then used to calculate AOD at 550 nm. This method effectively eliminates differences across spectral channels, enabling direct comparison of ground-based and satellite observations at a consistent wavelength.

The global distribution of AERONET sites, covering both land and ocean, together with its unified observation standards and strict quality control protocols, ensures consistency across sites worldwide. This provides a robust and comparable basis for validating satellite-derived AOD, thereby avoiding regional observational discrepancies and enhancing the global applicability of the validation results.

3. Study Area and Datasets

3.1. Experimental Data

To achieve effective fusion of multi-source data, unified spatiotemporal registration and quality control are first performed on the three Himawari AOD products and the MERRA-2 AOD product.

For Himawari products, the official quality flags are used directly for screening. The AOT_L2_Mean product retains all valid observations. For AOT_Merged and AOT_Pure products, only high-quality retrieval results are retained based on their respective QA flags. For the MERRA-2 product, as it is reanalysis data, all pixels are considered valid by default, requiring no additional screening. All three Himawari products are hourly data with a temporal resolution of 1 hour; MERRA-2 also provides hourly data with matching temporal resolution. Therefore, all data are directly aligned according to UTC time. Using the $0.05^\circ \times 0.05^\circ$ grid of the Himawari products as the unified spatial reference, the MERRA-2 product is resampled using the bilinear interpolation method to match the Himawari grid. During resampling, the four nearest original pixels around the target pixel are used, weighted according to distance, to obtain smooth and continuous interpolation results.

Through the above preprocessing, this study establishes a multi-source dataset with a unified spatiotemporal baseline ($0.05^\circ \times 0.05^\circ$ hourly), laying the foundation for Optimal Interpolation fusion. Subsequently, temporal and spatial collocation between AERONET and satellite AOD products is performed. Spatially, each AERONET site is matched to its corresponding satellite grid

cells by extracting a 3×3 neighborhood centered on the site, and the mean value of valid pixels within this window is compared with the ground measurement.

3.2. Optimal Interpolation Fusion

Optimal Interpolation is a statistical method widely used in data assimilation. Its core idea is to estimate the optimal weight matrix using the error covariance of the background field and observations under known conditions, minimizing the error variance of the analysis field [10]. In this study, the product with the highest accuracy is used as the background field. Subsequently, the remaining products are sequentially fused as observation fields according to their accuracy ranking. After fusing each product, the fused product is considered the new background field for the next pixel-wise fusion step.

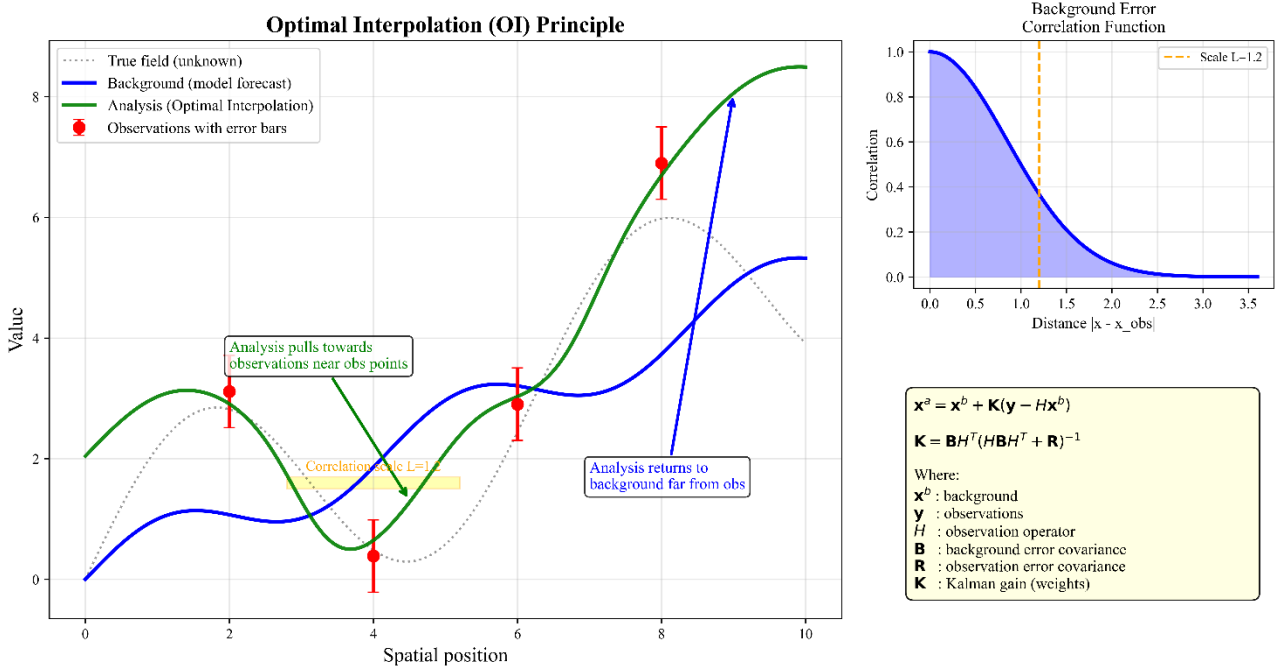


Figure 2: Schematic Diagram of Optimal Interpolation Fusion

The basic principle of Optimal Interpolation is shown in Figure 2. The fundamental formula is:

$$x_a = x_b + K(y - Hx_b) \quad (3)$$

Where x_a is the fused AOD value, x_b is the background field, y is the observation vector, and H is the observation operator. In this study, the background field and observation field are considered to be at the same location, and valid values are assumed not to be influenced by adjacent pixels; thus, H is considered to be 1. K is the Kalman gain matrix, calculated as:

$$K = BH^T(HBH^T + R)^{-1} \quad (4)$$

Here, B is the background field error variance, and R is the observation error variance. Since all products have been co-registered to the same grid, H can be considered the identity matrix, simplifying the gain matrix to:

$$K = \frac{B}{B + R} \quad (5)$$

For each pixel, the number N of valid observations from the three Himawari products at that

pixel is first counted. If $N \geq 1$, the product with the smallest error variance is selected as the primary observation value, the gain coefficient K is calculated, and the fused value is obtained. If $N = 0$, the MERRA-2 background field is directly used as the fusion result. The error variance for each product is calculated based on data matched with AERONET sites, reflecting the product's relative global accuracy.

To avoid speckle noise that might be introduced by single-pixel fusion, a 3×3 neighborhood spatial consistency constraint is further introduced to modify the fusion weights. Specifically, the variance of each product within the 3×3 neighborhood is calculated; a smaller variance indicates higher spatial consistency and thus a higher weight. The final fusion weight is determined jointly by the error variance and spatial consistency, as shown in the formula:

$$weight = \left(\frac{(\sigma_e^2)^{-1}}{\sum_i (\sigma_{e,i}^2)^{-1}} \right) \times \left(\frac{(\sigma_n^2)^{-1}}{\sum_j (\sigma_{n,j}^2)^{-1}} \right) \quad (6)$$

Where σ_e^2 is the error variance, and σ_n^2 is the neighborhood variance. This composite weighting strategy minimizes error while improving the spatial continuity of the fusion results.

3.3. Accuracy Validation Method

To comprehensively evaluate the accuracy of the fused product, this study uses global AERONET Level 1.5 site observations as ground truth for validation. The selected statistical indicators include the correlation coefficient (r), coefficient of determination (R^2), root mean square error (RMSE), bias (Bias), and the proportion within the Expected Error (EE) envelope.

$$r = \frac{\sum(y_i - \bar{y})(\hat{y}_i - \bar{\hat{y}})}{\sqrt{\sum(y_i - \bar{y})^2} \sqrt{\sum(\hat{y}_i - \bar{\hat{y}})^2}} \quad (7)$$

$$R^2 = 1 - \frac{\sum(y_i - \hat{y}_i)^2}{\sum(y_i - \bar{y})^2} \quad (8)$$

$$RMSE = \sqrt{\frac{1}{n} \sum(y_i - \hat{y}_i)^2} \quad (9)$$

$$Bias = \frac{1}{n} \sum(\hat{y}_i - y_i) \quad (10)$$

$$EE = \pm(0.05 + 0.15 \times y_i) \quad (11)$$

Here, y_i is the AERONET AOD observation value, and \hat{y}_i is the model or satellite product AOD value. The proportion of samples falling within the EE range intuitively reflects the reliability of the product.

4. Experimental Results and Discussion

4.1. Validation of Himawari Satellite AOD Products

The original satellite AOD data used in this section are the Himawari L3 hourly products, including the three aforementioned types: AOT_L2_Mean, AOT_Merged, and AOT_Pure. Their

hourly coverage rates were calculated and comparatively analyzed. As shown in Figure 3, the horizontal axis represents Coordinated Universal Time (UTC), the vertical axis represents the coverage percentage, and the three different curves represent the three products.

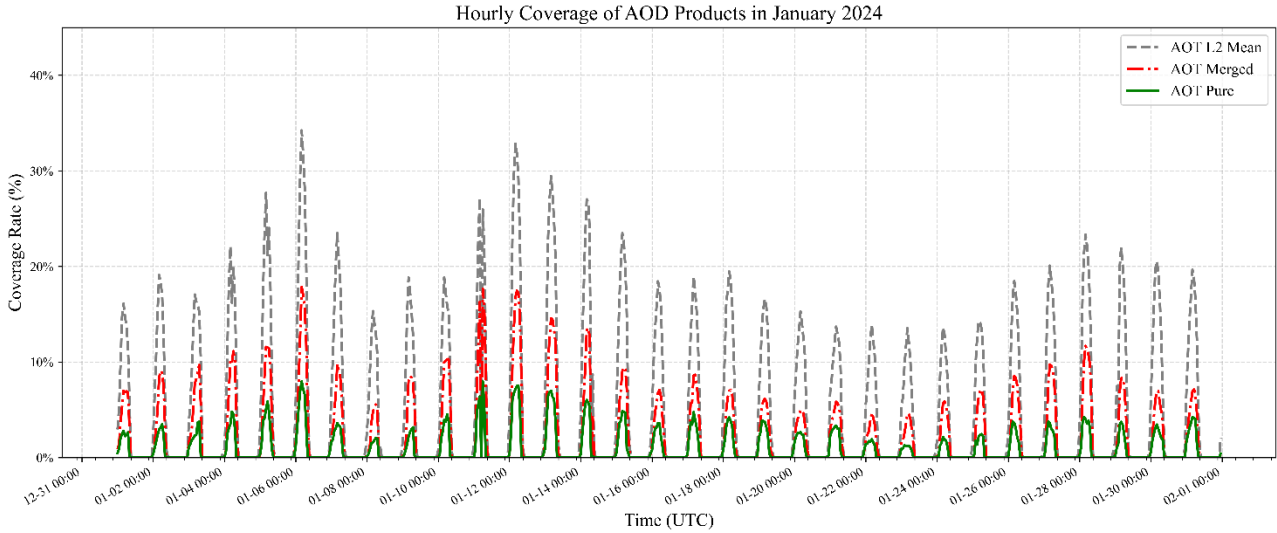


Figure 3: Time Series of Himawari AOD Product Coverage

Overall, the AOT_L2_Mean product exhibits the best coverage among the three. Its coverage generally fluctuates between 15% and 30% throughout January, mostly stabilizing above 20%, peaking near 35% around January 8. This result demonstrates the maximum detection capability of the Himawari satellite data. Without other post-processing of the data product, combining valid data within each hour yields a relatively high product coverage. Therefore, AOT_L2_Mean is the core product providing sufficient data samples.

The AOT_Merged product has the second-highest coverage, with an overall coverage level fluctuating between 10% and 25%, approximately 5 percentage points lower than AOT_L2_Mean. This reflects that the official fusion algorithm, while integrating satellite retrievals with climatological background information, performs preliminary data screening. Although this reduces the overall product coverage, it enhances product reliability.

The AOT_Pure product has the lowest coverage among the three, generally maintained between 5% and 20%, with several significant troughs in mid-to-late January. For example, it dropped below 5% around January 23. AOT_Pure is a higher-quality satellite retrieval result obtained by the official improved retrieval algorithm, representing high-quality retrieval values identified by the algorithm. However, this quality screening sacrifices substantial spatial coverage, especially in areas with frequent cloud cover, where the number of valid pixels is greatly reduced.

Regarding temporal variation characteristics, all three products exhibit significant diurnal periodic fluctuations. As the Himawari satellite is located in a geostationary orbit at 140.7°E, its observations over East Asia are significantly influenced by the solar elevation angle. During UTC 00:00 to 08:00, corresponding to 08:00 to 16:00 local time in East Asia (daytime hours), the coverage of all three products is generally high. Peaks usually occur around UTC 04:00-06:00, near local noon, when the solar elevation angle is maximum, cloud cover is relatively low, and retrieval conditions are optimal. Conversely, during UTC 12:00 to 20:00, corresponding to nighttime in East Asia, optical remote sensing cannot perform effective retrievals due to lack of sunlight, and the coverage of all three products drops sharply to near zero, forming daily data valleys.

Furthermore, Figure 3 also shows some day-to-day fluctuations in the coverage of the three products during January. For instance, between January 8 and 12, the coverage of all three products decreased noticeably, possibly related to widespread rainy weather processes in East Asia during

that period. In late January, the coverage fluctuation of the AOT_Pure product was particularly severe, reflecting the higher sensitivity of pure retrieval products to weather conditions.

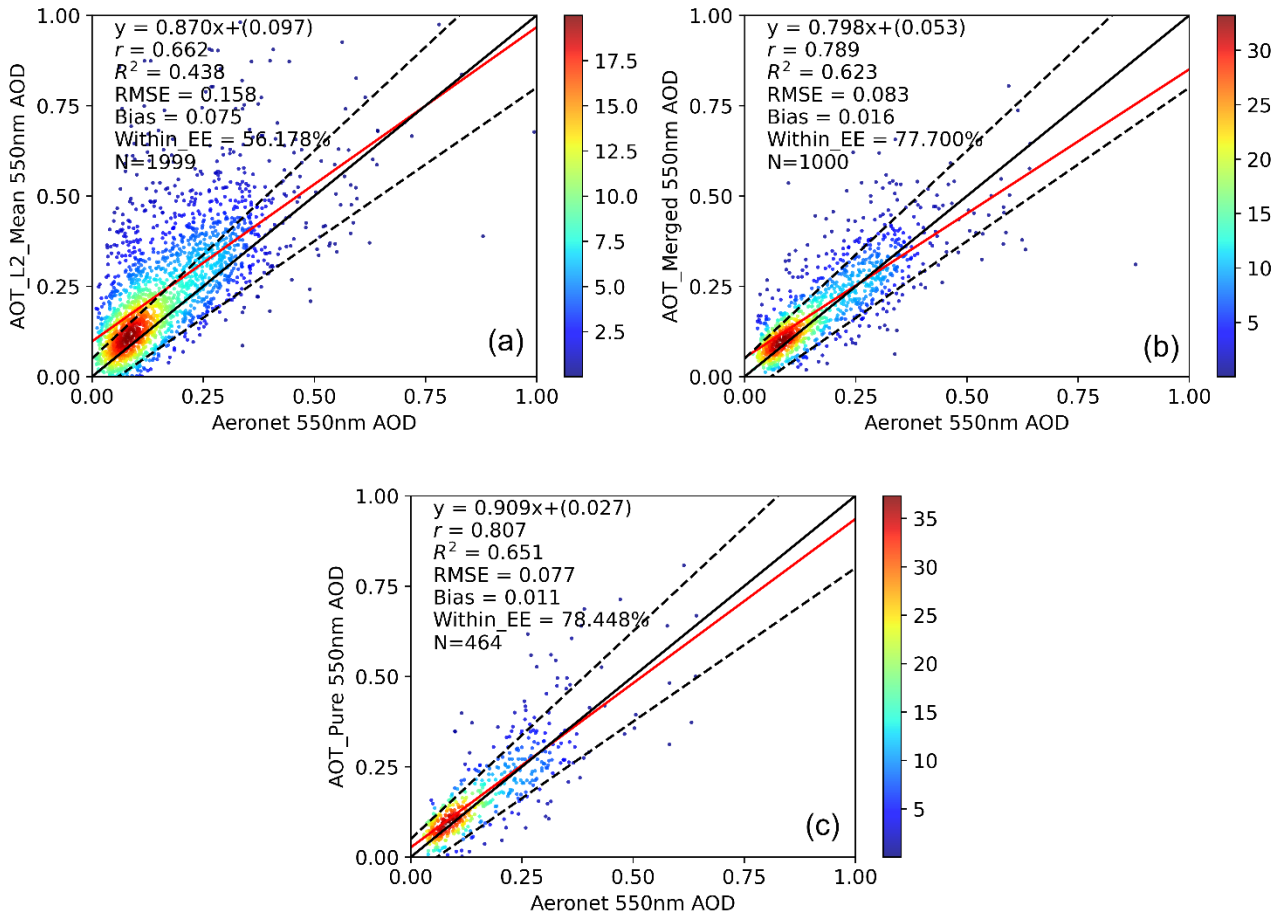


Figure 4: Accuracy Validation Results of Himawari AOD Products: (a) AOT_L2_Mean, (b) AOT_Merged, (c) AOT_Pure.

Overall, the AOT_L2_Mean product has a clear advantage in coverage. However, even for the product with the best coverage, its average coverage during daytime hours is only 20%-25%, and it is essentially zero at night. This situation fully demonstrates that relying solely on the official products of a single geostationary satellite is far from sufficient to meet the demand for continuous hourly AOD data, necessitating the use of reanalysis data to fill the missing areas.

The three products were further compared against AERONET site observations to analyze their accuracy. Figure 4 shows that in January 2024, the three Himawari AOD products generally exhibit a good linear correlation with AERONET observations within the study area, but there are significant differences in accuracy between different products. Overall, scatter points are mainly concentrated in the low AOD region, and high-density areas are clustered near the 1:1 reference line, indicating good consistency between satellite retrievals and ground-based observations under low aerosol load conditions. The red solid line indicates the regression fit, the black solid line is the 1:1 reference line, and the black dashed lines denote the EE envelope. The color scale represents sample density, with red indicating higher density and blue lower density.

Specifically, the AOT_L2_Mean product has a correlation coefficient r of 0.662, a coefficient of determination R^2 of 0.438, an RMSE of 0.158, a Bias of -0.075, and 56.178% of samples fall within the EE range, with a sample size of 1999. Although this product has the largest number of samples, its correlation is relatively low, its RMSE is large, and the negative Bias indicates a general

underestimation. Moreover, only about 56% of samples fall within the EE envelope, suggesting its retrieval accuracy is relatively limited.

The AOT_Merged product shows significantly improved correlation, with $r = 0.789$, $R^2 = 0.623$, RMSE reduced to 0.083, Bias = 0.016, and the proportion within EE reaching 77.700%, with a sample size of 1000. Compared with AOT_L2_Mean, the errors of this product are significantly reduced, and the Bias is close to zero, indicating small systematic bias, with most samples distributed within the EE range, showing a clear improvement in overall retrieval accuracy.

The AOT_Pure product exhibits the highest accuracy among the three. Its correlation coefficient r reaches 0.807, $R^2 = 0.651$, RMSE is further reduced to 0.077, Bias = 0.011, and the proportion within EE is 78.448%, with a sample size of 464. The fitted line for this product is closest to the 1:1 reference line, indicating the best consistency with AERONET observations. However, the number of valid samples for this product is relatively small, showing that while strict screening conditions improve retrieval accuracy, they reduce data coverage.

A comprehensive comparison of the three products reveals that AOT_Pure has the highest accuracy, followed by AOT_Merged, while AOT_L2_Mean has relatively lower accuracy but the largest sample size. This indicates that as quality control conditions become stricter, the reliability of AOD retrieval results increases significantly, but the number of available samples decreases simultaneously. Therefore, a trade-off between data accuracy and spatial coverage is necessary in practical applications.

4.2. Validation of MERRA-2 AOD Data Quality

Figure 5 presents the accuracy validation results of the hourly MERRA-2 AOD product against AERONET observations. The MERRA-2 product has a correlation coefficient $r = 0.617$, $R^2 = 0.380$, RMSE = 0.121, Bias = -0.013, and 71.63% of samples fall within the EE range, with a sample size also of 3162. The fitted slope for MERRA-2 is 0.447, with an intercept of 0.082. However, because the MERRA-2 AOD product is generated through model simulation, it possesses completeness and spatiotemporal continuity. Therefore, it can complement the three observation-based Himawari products, and through data fusion, an AOD field that balances accuracy and coverage can be obtained. The red solid line indicates the regression fit, the black solid line is the 1:1 reference line, and the black dashed lines denote the EE envelope. The color scale represents sample density, with red indicating higher density and blue lower density.

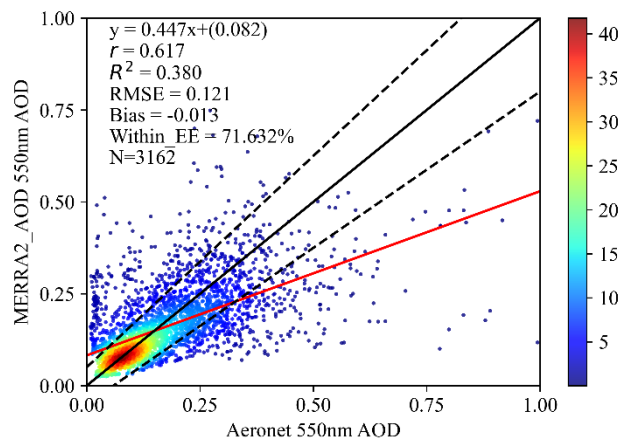


Figure 5: Accuracy Validation Result of Hourly MERRA-2 AOD Product.

4.3. Accuracy Assessment of Optimal Interpolation Fusion Results

After completing the hourly Optimal Interpolation fusion of the four products, a seamless hourly AOD product for the East Asian region was obtained. Figure 6 shows the matching validation results of the seamless hourly fused AOD product against AERONET ground-based observations. It can be seen that the fusion results have a certain correlation with the site observations. The correlation coefficient $r = 0.662$, $R^2 = 0.439$, RMSE = 0.118, Bias = 0.015, and the proportion of samples falling within the expected error envelope is 68.438%, with a sample size of 3162. Overall, the final result maintains a certain level of accuracy while ensuring 100% continuous coverage. Meanwhile, the fitted slope is 0.556, and the intercept is 0.092. It can be observed that, influenced by the four original products, the fusion results still exhibit some degree of underestimation and high-value compression. The red solid line indicates the regression fit, the black solid line is the 1:1 reference line, and the black dashed lines denote the EE envelope. The color scale represents sample density, with red indicating higher density and blue lower density.

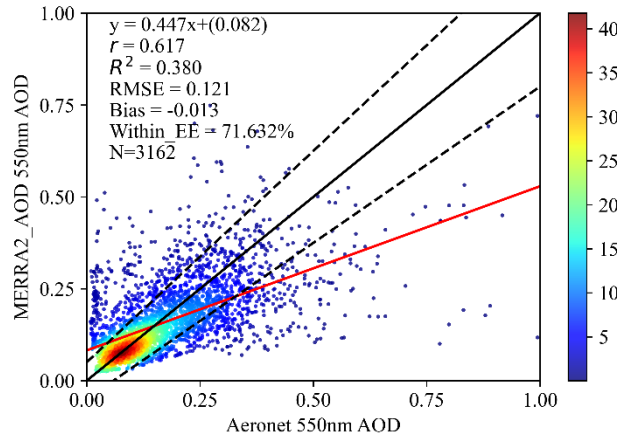


Figure 6: Accuracy Validation Result of Hourly Optimal Interpolation Fusion Product.

Comparing the final fusion result with MERRA-2 AOD, in terms of validation accuracy against AERONET, by introducing the three Himawari observation products for constraint, the accuracy of the final fusion product is improved compared to the MERRA-2 product. For hourly AOD detection, the MERRA-2 product also has a limited ability to respond to local high values and rapid fluctuations on an hourly scale. In contrast, although the optimal interpolation fusion result from this study is slightly inferior to MERRA-2 in overall statistical indicators, its spatial distribution simultaneously captures the detailed features of the original Himawari observations, retaining relatively richer local structural information.

Figure 7 shows the coverage of the original Himawari AOT_L2_Mean hourly AOD product. It can be seen that, affected by cloud cover and retrieval condition limitations, the original product has numerous irregular gaps during daytime hours. Additionally, it shows systematic overall absence at night due to the lack of visible light observation conditions. This missing data characteristic severely impacts AOD time series analysis and pollution process identification. It can be observed that from UTC 09:00 to 23:00, the study area is essentially in a nighttime state, during which AOD detection is impossible.

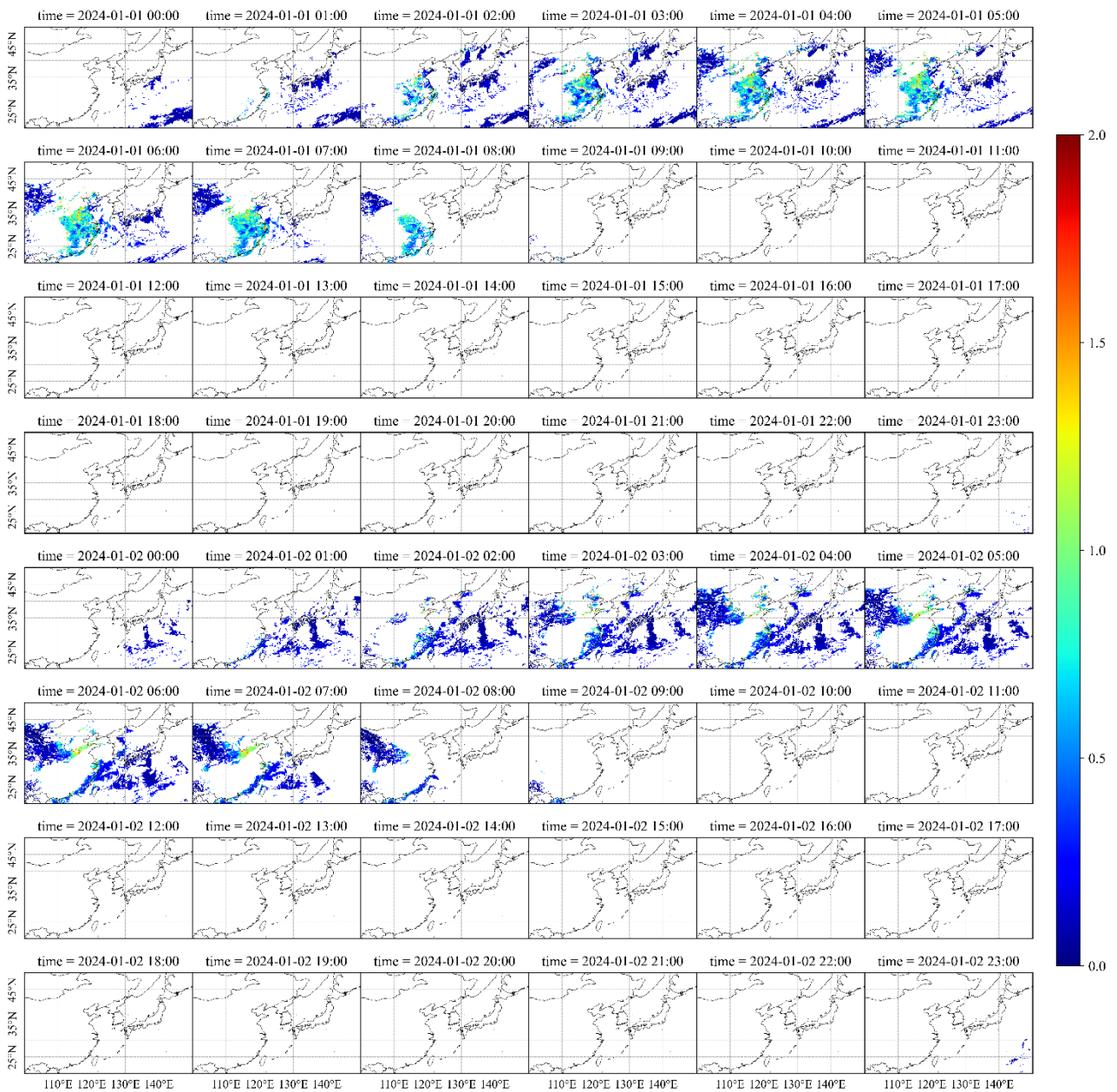


Figure 7: Hourly Himawari AOD Coverage Map

In contrast, after fusion of multi-source data, the hourly AOD product achieves spatially continuous coverage at all times, significantly improving data completeness and usability. On one hand, the AOD distribution in daytime cloud-covered areas is effectively complemented. On the other hand, estimated results with spatial structure constraints are also obtained for nighttime periods without observations, thus extending the originally discrete hourly observations into a continuous hourly AOD spatiotemporal sequence.

Figure 8 displays the seamless hourly AOD fusion map. In terms of spatial distribution, high AOD areas over the East Asian continent still retain relatively clear pollution belts and regional gradient features in the fusion results, while oceans and clean background areas show relatively low and smooth AOD values, generally consistent with the typical patterns of regional aerosol distribution.

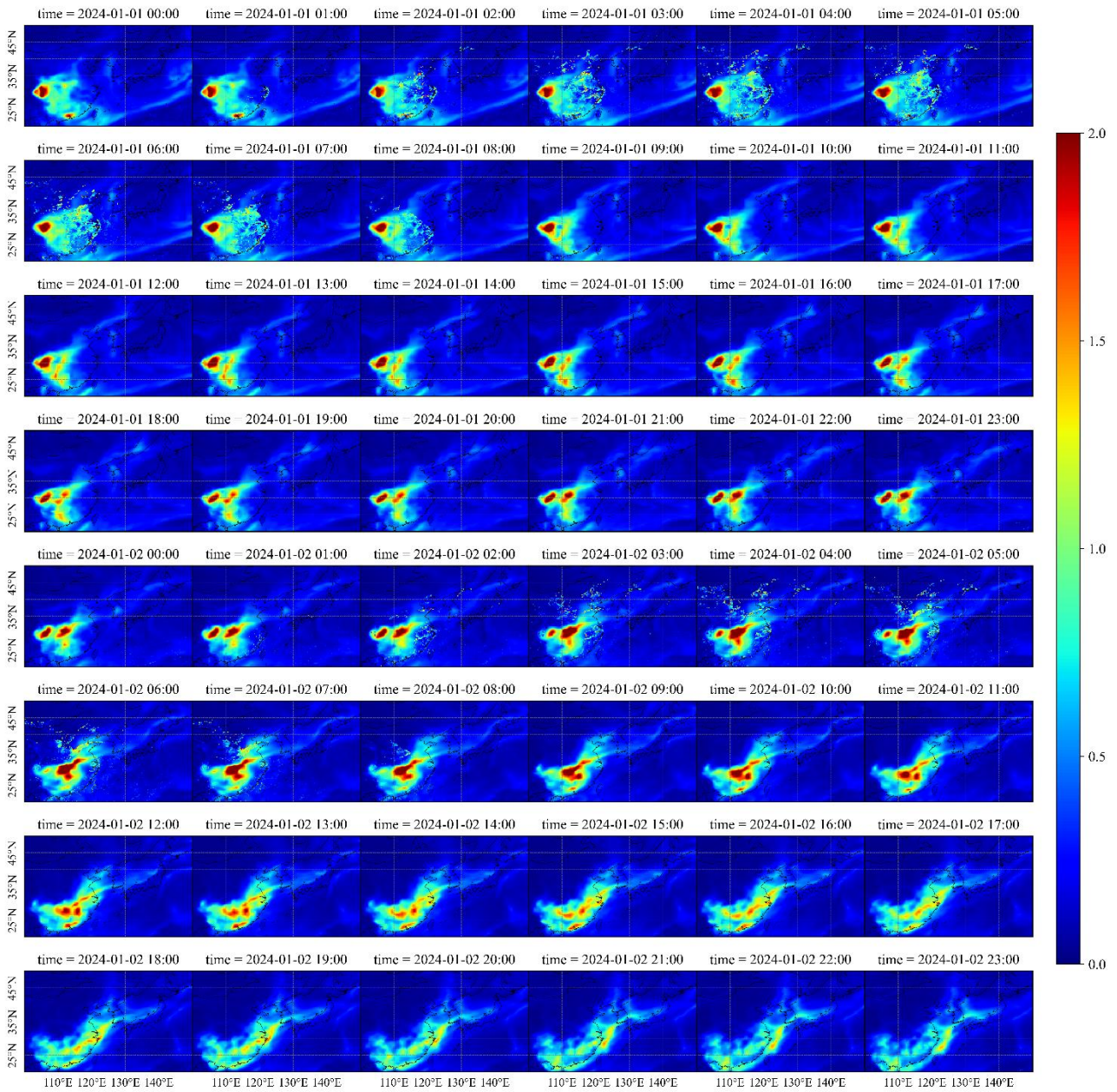


Figure 8: Seamless Hourly AOD Fusion Map

Although the fused AOD product achieves seamless coverage, its quality in large gap areas and regions completely unobserved at night cannot be guaranteed. From the current results, for large gaps and completely unobserved nighttime areas, the product primarily relies on the AOD background field provided by MERRA-2, as the limited available Himawari data cannot play a role in such scenarios. Therefore, overall, for AOD research at the hourly scale, sufficiently abundant effective satellite detection remains one of the most critical factors.

Overall, the seamless hourly AOD fusion based on Himawari satellite and reanalysis data constructed in this paper can solve the problem of large-scale missing data in geostationary satellite AOD products during daytime cloud-covered areas and nighttime periods, achieving complete fusion in gap regions. Its overall accuracy is better compared to the single atmospheric model simulation reanalysis data, while simultaneously leveraging the quality assurance of satellite observation data and the spatiotemporal continuity of reanalysis data. Through the optimal

interpolation fusion design combining Himawari satellite observations and MERRA-2 reanalysis data, a complete AOD product can be fused. This can also provide reference basic data for pollution process identification and regional air quality dynamic monitoring.

5. Conclusion

This study investigates the seamless fusion of hourly AOD using Himawari satellite AOD products and MERRA-2 reanalysis data. It aims to leverage the complementary advantages of satellite observations and reanalysis data, fully utilizing the high temporal resolution continuous observation capability of geostationary satellites and the spatiotemporal continuity of reanalysis data to construct a seamless AOD product capable of reflecting regional aerosol variation processes on an hourly scale.

This paper validated the accuracy and analyzed the coverage of the three Himawari L3 AOD products and the MERRA-2 AOD product. Based on the validation results for each product, their respective validation accuracies were used as weights to perform Optimal Interpolation fusion on the four products, resulting in a seamless hourly AOD fusion product. While ensuring spatiotemporal seamlessness, the fused product achieved validation metrics against AERONET of $r = 0.662$ and $RMSE = 0.118$, balancing reasonable accuracy with spatiotemporal continuity.

Current research is still limited by the quality and quantity of data sources. Future work could investigate more geostationary satellite AOD products and attempt to reconstruct missing data using machine learning methods. Additionally, the current experimental data is focused on January 2024; future studies will explore longer time series data to investigate the seasonality and periodicity of AOD variations.

In summary, this research expands the multi-source seamless fusion work for hourly-scale AOD, validates the applicability of fusion based on satellite observation data and reanalysis data, and provides a data foundation for pollution process identification and regional air quality dynamic monitoring.

Acknowledgements

This work was supported by the project "Integration and Demonstration Technology of Transparent Earth-Observing" (Grant No. 2023YFB3907705). The author also extends sincere gratitude to the editors and anonymous reviewers for their valuable contributions.

References

- [1] Rosenfeld D ,Lohmann U ,Raga B G , et al. Flood or Drought: How Do Aerosols Affect Precipitation?[J].*Science*,2008,321(5894):1309-1313.DOI:10.1126/science.1160606.
- [2] ZHANG T, SHEN H, XIA X, et al. 2023. Himawari-8 High Temporal Resolution AOD Products Recovery: Nested Bayesian Maximum Entropy Fusion Blending GEO With SSO Satellite Observations[J/OL]. *IEEE Transactions on Geoscience and Remote Sensing*, 61: 1-15. DOI:10.1109/TGRS.2023.3262785.
- [3] Feng L , Su X , Wang L ,et al. Accuracy and error cause analysis, and recommendations for usage of Himawari-8 aerosol products over Asia and Oceania[J]. *Science of The Total Environment*, 2021, 796(12):148958. DOI:10.1016/j.scitotenv.2021.148958.
- [4] Yunhui T ,Quan W ,Zhaoyang Z .Assessing spatiotemporal variations of AOD in Japan based on Himawari-8 L3 V31 aerosol products: Validations and applications[J]. *Atmospheric Pollution Research*, 2022, 13(6): DOI:10.1016/J.APR.2022.101439.
- [5] Chatterjee A ,Michalak M A ,Kahn A R , et al. A geostatistical data fusion technique for merging remote sensing and ground-based observations of aerosol optical thickness[J].*Journal of Geophysical Research: Atmospheres*, 2010, 115(D20): DOI:10.1029/2009JD013765.
- [6] Ronald G ,Will M ,J M S , et al. The Modern-Era Retrospective Analysis for Research and Applications, Version 2 (MERRA-2).[J].*Journal of climate*,2017,30(13):5419-5454.DOI:10.1175/JCLI-D-16-0758.1.

- [7] Singh S ,Singh A ,Srivastava K A , et al. *Assessment of Surface PM2.5 Concentrations over India using Modern-Era Retrospective Analysis for Research and Applications, Version 2 (MERRA-2) Reanalysis Data*[J].*Pure and Applied Geophysics*,2025,182(4):1-23.DOI:10.1007/S00024-025-03666-6.
- [8] Holben B N , Eck T F , Slutsker I ,et al. *AERONET—A Federated Instrument Network and Data Archive for Aerosol Characterization*[J].*Remote Sensing of Environment*, 1998, 66(1):1-16.DOI:10.1016/S0034-4257(98)00031-5.
- [9] Eck T F , Holben B N , Reid J S ,et al. *Wavelength dependence of the optical depth of biomass burning, urban, and desert dust aerosols*[J].*Journal of Geophysical Research Atmospheres*, 1999, 104(D24):31333-31349. DOI:10.1029/1999JD900923.
- [10] Carnevale C , De Angelis E , Finzi G ,et al. *Optimal Interpolation Based Data Fusion Techniques to Improve Deterministic Air Quality Forecast*[C]//*International Technical Meeting on Air Pollution Modelling and its Application*. Springer, Berlin, Heidelberg, 2021.DOI:10.1007/978-3-662-63760-9_22.